The United Nations University

GEOTHERMAL TRAINING PROGRAMME
Orkustofnun, Grensásvegur 9,
IS-108 Reykjavík, Iceland

Reports 2005
Number 15

PRELIMINARY DESIGN OF A PROPOSED GEOTHERMAL POWER PLANT IN NW-SABALAN AREA, AZERBAIJAN-IRAN

Behnam Radmehr
SUNA – Renewable Energy Organization of Iran
Yadegare Emam Highway, Poonake Bakhtari Ave., Shahrake Ghods
P.O.Box 14155-6398, Tehran
IRAN
radmehr.beh@gmail.com

ABSTRACT

Mt. Sabalan geothermal field is a high-temperature area under development. The first exploration wells have been drilled in the northwest area and shown it to be a water-dominated system. Well–pad B includes production wells NWS-4 and NWS-5R and will also accommodate additional production wells. Plans are underway to develop a power plant at well-pad B by using the available resource from these wells. The main objectives of this paper are to design and to determine the optimum parameters for the technical operation of the system and optimize the electrical power production process. It has been assumed that the properties of five additional wells are the same as those of the existing well, NWS-4. The steam condensing cycle combined with a binary ORC was selected as the power generation system. The obtained results show that based on these assumptions the highest power output from a steam condensing plant alone can be 19.5 MWe with 3 and 0.08 bar-a for separator and condenser pressures, respectively. But the optimum output power from a combined steam and binary plant has been calculated as 26.2 MWe.

1. INTRODUCTION

1.1 General problem description

The Renewable Energy Organization of Iran - SUNA has identified a potentially viable geothermal resource at Mt. Sabalan, in the Azerbaijan region of NW-Iran. The long-term target capacity of electrical power generation in the NW-Sabalan project is expected to be 100 MWe. There are several development scenarios available to reach the target capacity with different power plant configurations at existing locations and different unit capacity. Steam-field and power plant options at the Mt. Sabalan development site are constrained by the difficulties in crossing deep and steep-sided gullies. Well-pad B is preferred for early development in order to avoid the need for pipelines to cross a steep gully and unstable terrain. Well-pad B includes production wells NWS-4 and NWS-5R and can also accommodate additional four production wells with deep cellars. In this report, power generation from wells on pad-B is considered.

1.2 Literature review

The following summarizes conclusions obtained by some previous investigations into geothermal power plants, related matters and problems.

Kanoglu (2001) showed that when using low-temperature resources, geothermal power plants generally have a low first-law efficiency. This means that more than 90% of the energy of the geothermal water is discarded as waste heat. There is a strong argument here for the use of geothermal resources for direct applications such as district heating instead of power generation, when economically feasible. When considering binary geothermal power plants using air as the cooling medium, the condenser temperature varies as the ambient air temperature fluctuates throughout the year and even throughout the day. As a result, power output decreases by up to 50% from winter to summer.

Valdimarsson (2003) concluded by analysis, that the Carnot efficiency is not valid as a reference for electrical power generation from low-temperature sources. The energy and exergy contained in the stream *m* has to be considered waste, if this energy cannot be sold as heat. The only valid reference for the efficiency of a pure electricity plant is to maximize the first-law efficiency when electricity is the sole output of the plant. If the heat in the stream can be sold, the whole mass flow is a by-product of the power plant, and irrelevant to the power plant itself. Maximum electrical production efficiency, in this case, is presented as combined heat and power production.

Mineral Processing Research Institute (2001) indicates that shell and tube heat exchangers represent the most widely used equipment for the transfer of heat in industrial processing applications. Shell and tube heat exchangers have the ability to transfer large amounts of heat at relatively low cost and serviceable designs. They can provide large amounts of effective tube surface while minimizing the requirements of floor space, liquid volume and weight. Shell and tube exchangers are available in a wide range of sizes. They have been used in the industry for over 150 years, so the thermal technologies and manufacturing methods are well defined and applied by modern competitive manufacturers. Tube surfaces range from standard to exotic metals with plain or enhanced surface characteristics widely available. They can help provide the least costly mechanical design for the flows, liquids and temperatures involved.

Gudmundsson (1983) indicates that quartz and amorphous silica are of interest in deposition studies. In liquid-dominated high-temperature geothermal reservoirs, the amount of silica dissolved in the geothermal water depends on the solubility of quartz. However, amorphous silica precipitates from geothermal fluids upon concentration and cooling. Silica deposition and scaling will occur in geothermal wells and surface facilities when the concentration of silica exceeds the solubility of amorphous silica.

Sanyal (2005) has noticed that the power cost is sharply reduced for at least the first 10 years of operation if full generation capacity is maintained, by drilling additional wells. However, continuing make-up well drilling beyond about 20 years does not reduce power cost any further. The minimum achievable power cost is insensitive to plant capacity; it is on the order of 3-4 US¢ / kWh.

1.3 General information about the Mt. Sabalan geothermal field

The Mt. Sabalan – Meshkin Shahr geothermal field is located in the vicinity of the Moil Valley on the northwest flank of Mt. Sabalan, in the Meshkin Shahr town (Khiyav) of Azerbaijan, Iran. The resource area has been previously identified by geo-scientific studies as an approximately quadrangular shaped area that covers approximately 75 km^2.

The geothermal field is located in an environmentally sensitive area of elevated valley terraces set within the outer caldera rim of the greater Mt. Sabalan complex. Mt. Sabalan is a Quaternary volcanic complex that rises to a height of 4811 m, some 3800 m above the Ahar Chai valley to the north. Volcanism within the Sabalan caldera has formed three major volcanic peaks which rise to elevations of around 4700 m. The climate in the area is relatively dry, especially during the summer months. The site is exposed to severe winter weather, including very high wind speeds of up to 180 km/hr. Winter temperatures over the past 4 years have been measured as low as - 30°C (SKM, 2005).

1.4 Purpose of this study

The main objectives of this study are to design and determine the optimum parameters for the technical operation of the system and optimize the electrical power production process suitable for well-pad B in the NW-Sabalan project. In this study, it has been assumed that the additional wells will have the same thermodynamic properties as those of existing well NWS-4. A steam-condensing unit combined with binary ORC is selected for the power plant system. Steam pipelines between the separator station and steam plants and the pipelines for the brine to the binary plant will be designed in this study. Cost estimation for the power plant system will also be discussed in this report.

2. EXPLORATION OF THE MT. SABALAN GEOTHERMAL AREA

2.1 Geology

Mt. Sabalan lies on the South Caspian plate, which is underthrust by the Eurasian plate to the north. It is, in turn, underthrust by the Iranian plate, which produces compression in a northwest direction. This is complicated by a dextral rotational movement caused by northward underthrusting of the nearby Arabian plate beneath the Iranian plate. There is no Benioff-Wadati zone to indicate any present day subduction. The current project area is located within the Moil Valley which, on satellite and aerial photograph imagery, can be seen to be a major structural zone. Exposed at the surface in the valley are altered Pliocene volcanics, an unaltered Pleistocene trachydacite dome (Ar-Ar date at 0.9 Ma) and Quaternary terrace deposits (Bogie et al., 2000). These units have been divided into four major stratigraphic units which, in order of increasing age, are (SKM, 2005):

- Quaternary alluvium, fan and terrace deposits.
- Pleistocene post-caldera trachyandesitic flows, domes and lahars.
- Pleistocene syn-caldera trachydacitic to trachyandesitic domes, flows and lahars.
- Pliocene pre-caldera trachyandesitic lavas, tuffs and pyroclastics.

The schematic geological map (Figure 1) shows the volcanic formations from Eocene to Quaternary.

2.2 Geochemistry

Warm springs and hot springs with Cl-SO_4, and SO_4 chemistries are found within the valley (Bogie et al., 2000). These plot in the immature area of the Na-K-Mg plot giving geo-thermometry temperatures of approximately 150°C (SKM, 2005). One of these, the Gheynargeh (Qeynerce) spring has a Cl concentration of 1800 mg/kg. Tritium analyses of this spring water indicate no recent interaction with the atmosphere.

The isotopic composition of the spring waters and their seasonal variations in flow, with little change in temperature or chemistry, suggest that a large regional groundwater aquifer overlies the potential geothermal reservoir.

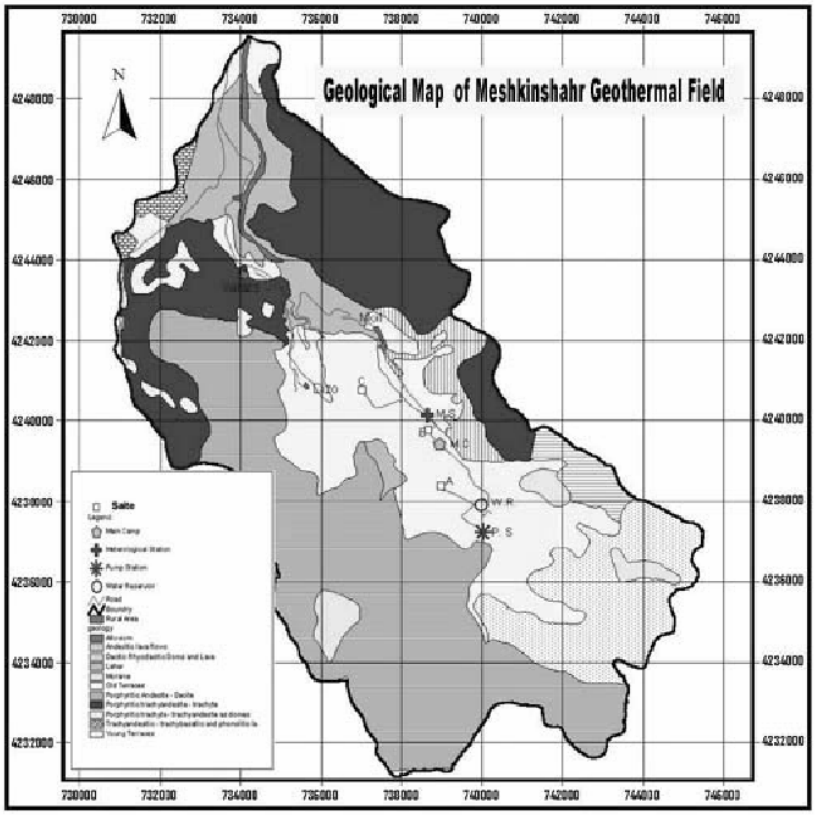

FIGURE 1: Geological map of the Meshkin Shahr area (Noorollahi and Yousefi, 2003)

2.3 Geophysics

A magnetotelluric (MT) survey (Bromley et al., 2000) established the existence of a very large zone of low resistivity (≈70 km^2) in the project area. Satellite imagery interpretation identified a large area (≈10 km^2) of surficial hydrothermal alteration in lower elevation parts of the project area, with much of the low-resistivity area in the valley covered by Quaternary terrace deposits. The presence of surficial hydrothermal alteration was confirmed by fieldwork. XRD analyses of this alteration revealed the presence of interlayered illite-smectite clays (which are conductive and will have formed at depth) indicating that at least some of the alteration and the resistivity anomaly are relics. At higher elevations unaltered rocks cover the zone of low resistivity. To define a target area for drilling, an area of very low resistivity (< 4 Ωm) associated with the thermal features was selected.

The early interpretation of the MT work (Bromley et al., 2000) shows low resistivities persisting to depth. However, once the relatively shallow occurrence of the conductive smectitic clays was established from the exploration geothermal wells, the MT data was reinterpreted in terms of the elevation of the base of the conductor. A conductive zone increasing in elevation to the south can be partially distinguished from the much larger and deeper resistivity anomaly to the west. This new interpretation is indicative of the current system's upflow occurring south of the drilled wells (Talebi et al., 2005).

2.4 Exploration drilling programme

On the basis of the results of the MT survey and the presence of hot springs with significant Cl concentrations, a three well exploration programme was undertaken. The topography of the valley limits the location of drill pads to interconnected terraces, requiring two of the wells to be directionally drilled to access the extensive anomaly at depth. The drilling and testing programmes were carried out between November 2002 and December 2004. The location of the project along with a detailed map of the drilled area, is given in Figure 2. The 3 deep exploration wells that have been drilled are coded NWS-1, NWS-3 and NWS-4 and these were drilled on well-pads A, C and B, respectively. The wells vary in depth from 2265 to 3197 m MD. Well NWS-1 was drilled vertically while NWS-3 and NWS-4 are directional wells with throws of 1503 and 818 m, respectively. Additionally, two shallow injection wells were drilled to 600 m depth, NWS2R located on pad A alongside well NWS-1 and NWS-5R on pad B alongside well NWS-4. The basic well completion data are summarised in Table 1.

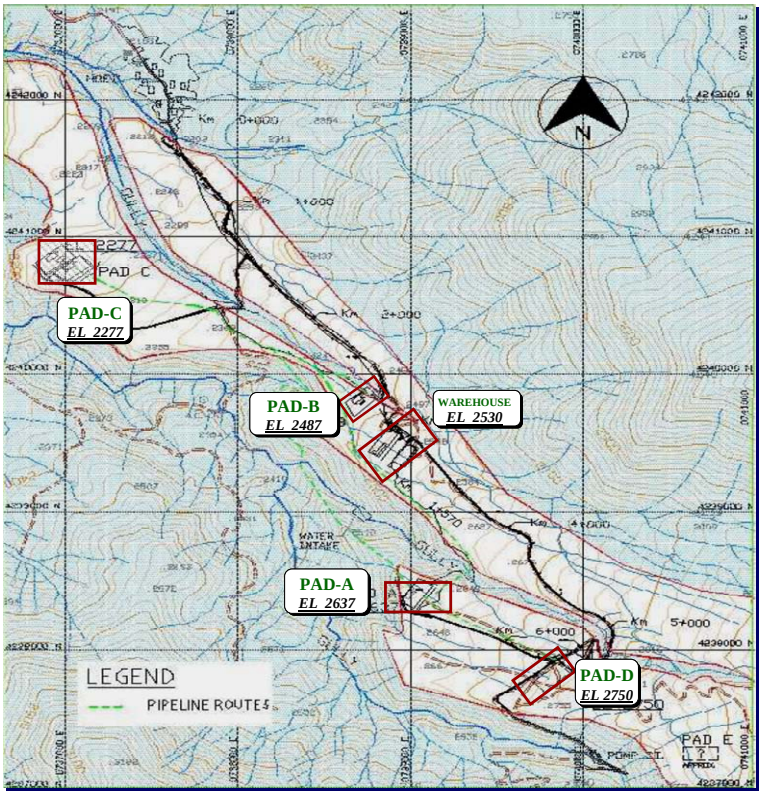

FIGURE 2: Topographic map of NW-Sabalan geothermal project area

TABLE 1: Basic completion information of NWS wells in Sabalan field (SKM, 2005)

Well	Spud date	Completion date	Depth MD / VD (m)	Prod. casing		Prod. liner	
				Size (in)	Depth (m MD)	Size (in)	Depth (m MD)
NWS-1	22 Nov 02	1 Jun 03	3197	9⅝	1586	7	3197
NWS-3	2 Jul 03	27 Nov 03	3166 / 2603	13⅜	1589	9⅝	3160
NWS-4	17 Dec 03	27 Mar 04	2255 / 1980	9⅜	1166	7	2255
NWS-2R	7 Jun 03	25 Jun 03	638	13⅜	360	9⅝, 5	638
NWS-5R	7 Apr 04	2 May 04	538	20	139	9⅝	482

2.5 Well testing and reservoir results

Well NWS-4 was discharged by airlift stimulation in September 2004 and a flow test carried out for the following 4 months with re-injection of waste brine into shallow well NWS-5R.

Output curves for well NWS-4 are shown in Figure 3 with output data from well NWS-1 also included for comparison. These show variations in total mass and enthalpy with flowing wellhead pressure. Both wells discharged with enthalpies in the range of 950-1000 kJ/kg, which is consistent with production from liquid-only feed zones with temperatures of 230°C (for NWS-1) and 220°C (for NW-3). These are both lower than the maximum temperatures measured in the two wells, 245 and 230°C, respectively.

Due to the relatively low overall permeability, the discharge of well NWS-1 is sensitive to wellhead pressure variation and flow could not be sustained at wellhead pressures above 4.5 bar-g. In contrast, well NWS-4, with a significantly higher permeability, showed a constant enthalpy of 950 kJ/kg at all wellhead pressures, reflecting the dominance of the 1620 m feed zone, and progressive decline in total flow and steam flow up to 10 bar wellhead pressure.

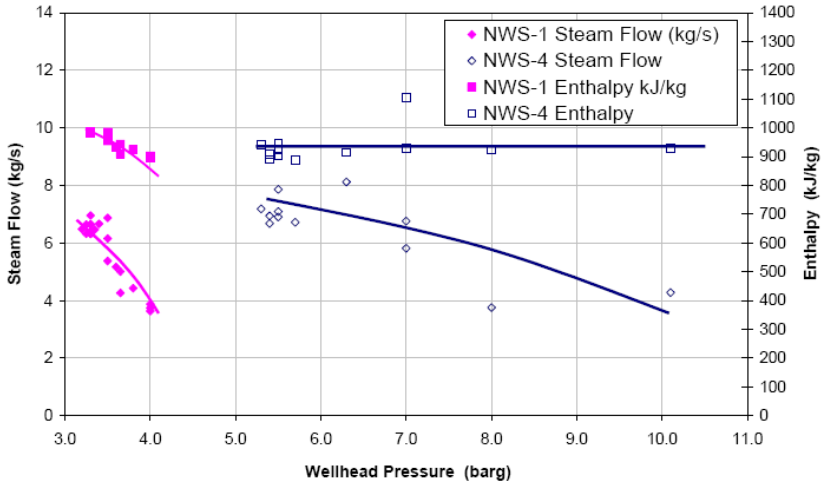

FIGURE 3: Output curve for well NWS-4

2.6 Well geochemistry

Full suites of brine and steam samples were collected from NWS-4 during the discharge test. Chemical analyses of these samples are presented in Table 2. The reservoir fluids produced by this deep well are slightly alkaline, relatively dilute, sodium chloride brines with TD chloride concentrators of about 2000 mg/kg and with approx 0.5% TDS. The concentration of CO_2 and H_2S in separated steam averages 2%, which is a typical value for developed geothermal fields.

TABLE 2: Summary of geochemistry, wells NWS-1 and NWS-4 (SKM, 2005)

Sabalan Wells - Brine Analyses:															
Well	**Date**	**Type**	**C.P.**	**pH**	**Li**	**Na**	**K**	**Ca**	**Mg**	**Fe**	**Cl**	**SO_4**	**$tHCO_3$**	**B**	**SiO_2**
			b.g.					*mg/kg*							
NWS1	14-Jun-04	SPW	2.4	8.88	8.3	1414	257	15	0.11	0.10	2411	117	105	22	520
NWS1	15-Jun-04	SPW	2.5	8.70	8.1	1402	254	15	0.10	0.05	2375	117	113	22	519
NWS1	16-Jun-04	SPW	3.1	8.56	8.1	1382	255	14	0.09	0.02	2336	118	130	21	506
NWS1	18-Jun-04	SPW	3.0	8.63	8.2	1385	252	14	0.09	0.04	2384	114	115	21	522
NWS4	13-Sep-04	WBX	0.0	8.60				31			2606	123	75	22	418
NWS4	14-Sep-04	ATM	0.0	8.39				31			2482	109	85	21	444
NWS4	15-Sep-04	ATM	0.0	8.42				31			2500	100	85	22	466
NWS4	16-Sep-04	SPW	1.5	8.42				26			2570	116	78	22	484
Analyses for NWS-4 incomplete at time of going to press															

Sabalan Wells - Steam Gas Analyses, Molar Ratios and Brine Geothermometry:													
Well	**Date**	**Type**	**C.P.**	**CO_2**	**H_2S**	**Cl**	**Cl**	**Cl**	**Na**	**Cl_{RES}**	**T_{QTZ}**	**T_{NaK}**	**CO_2**
				mM/100M		—	—	—	—				—
			b.g.	*@ SCP*		**Ca**	**B**	**SO_4**	**K**	*mg/kg*	°C	°C	**H_2S**
NWS1	14-Jun-04	SPW	2.4	917	5.8	185	33	56	9.4	2030	238	266	158
NWS1	15-Jun-04	SPW	2.5	860	3.8	185	33	55	9.4	1991	238	266	226
NWS1	16-Jun-04	SPW	3.1	1002	4.9	189	34	54	9.2	2005	237	267	204
NWS1	18-Jun-04	SPW	3.0			195	35	57	9.3	2050	239	267	
NWS4	13-Sep-04	WBX	0.0			95	37	57		1992	215		
NWS4	14-Sep-04	ATM	0.0	756	6.2	91	35	62		1897	219		122
NWS4	15-Sep-04	ATM	0.0			91	35	68		1911	223		
NWS4	16-Sep-04	SPW	1.5	742	4.6	112	36	60		2065	230		161

Notes: CP = Collection pressure, SPW = separated water, ATM = at atmospheric pressure, WBX= silencer weirbox, b.g. = pressure in bars gauge

Silica geothermometry shows NWS-4 brine yields silica temperatures of up to 235°C, equivalent to liquid water at 1010 kJ/kg. This temperature estimate is close to the maximum temperature measured in the well but the enthalpy is somewhat higher than the actual discharge enthalpy. Cation geothermometer temperatures for NWS-1 fluids, in the range 265-267°C, are therefore significantly higher than temperatures measured in the well. It is expected that well NWS-4 will also show high cation geothermometer temperatures when chemical analyses have been completed (SKM, 2005).

3. MT. SABALAN DEVELOPMENT OPTIONS

The target development capacity for the Sabalan project is about 100 MWe. Steam field and power plant options at the Sabalan development site are constrained by the difficulties in crossing the deep and steep-sided gullies that have incised into the valley floor. An early development, if considered appropriate, could be readily accommodated in the immediate vicinity of pads A or B, although pad B may be preferred in order to avoid the need for pipelines to cross a steep gully and unstable terrain immediately below pad A. Development on pad B would also take advantage of existing warehouse and laydown areas and should be able to accommodate a power plant of up to 20 MWe capacity. The route for a brine pipeline to the preferred injection well location at pad C is particularly straightforward and presents very few difficulties.

A first stage development in the vicinity of pad B, with a capacity of 20 MWe, would leave pad A available for a potentially larger development, depending on the results of proposed drilling at pad D and E. One option with 20 MWe provides for the two-phase production wells at site B with a separator station adjacent to the production well-pad to reduce pressure losses. Steam will be led to the nearby power plant and brine will be led to well-pad C to a binary power plant and re-injection wells. In this case, the pipe route for brine is straightforward. The elevation difference is approximately 200 m and the pipeline length is around 1.5 km over a relatively easy terrain.

3.1 Well requirements

The proposed steam field arrangements use existing well-pads A, B and C as well as proposed additional well-pads D and E. Each well-pad was assumed to be able to accommodate up to six wellheads. The validity of these assumptions and the suitability of the proposed new well-pads can be verified only when further geophysical studies are completed and additional wells have been drilled and tested. In order to determine possible steam field layouts for development options, it was necessary to consider the proximity of potential power plant sites to the existing and prospective well-pads. There are few constraints to the locations of power plant sites. For this reason we have assumed that the power plants sites will be readily developed adjacent to the current and prospective production well-pads. The following exploration well-pads have been considered:

- Well-pad A includes existing wells NWS-1 and NWS-2R. With the scheduled deep-cellar construction, pad A will accommodate additional four wells.
- Well-pad B includes wells NWS-4 and NWS-5R and will also accommodate additional four deep-cellar production wells. Developed platforms just above this site, currently used for drilling materials and warehousing, are capable of accommodating a power plant of up to 100 MWe capacity.
- Well-pad C is at the lowest elevation and is regarded as being on the outer edge of the reservoir. Well NWS-3 drilled from well-pad C, and currently reserved for brine re-injection, can readily accommodate additional brine re-injection wells. There is more than adequate area available in the immediate vicinity to well-pad C for a binary power plant.

Prospective total power generation capacity (100 MWe), number of new wells and steam field layout for this target that involve the production of steam from well-pads D, E and F, are speculative.
The maximum injection rate for new injection wells is assumed to be 75 kg/s (SKM, 2005). The number of injection wells required for each of the development options could be obtained by rounding up the total excess condensate divided by the estimated maximum injection rate (75 kg/s).

4. THEORY AND METHOD OVERVIEW

4.1 Steam field

Exploration data of the NW-Sabalan geothermal field show that this field is a liquid-dominated system. The known resources show that water is available at a temperature of around 230°C. Because the wells are non-artesian they must be stimulated to initiate flow. When discharged, the water flows naturally under its own pressure. The drop in pressure causes it to partially flash into steam and arrive at the wellhead as a two-phase mixture.

The geothermal fluid is flashed into steam as the hydrostatic column is reduced to a sustained wellhead pressure. Steam will be supplied from wells on pad B to the power plant. As has been already mentioned, one production well on pad B is available and the pressure, temperature, enthalpy, mass flow and chemical characteristics of its fluid have been identified through testing. When wellhead pressure is 8.25 bar-a, the two-phase mass flow from the well is 50 kg/s with an enthalpy of 954 kJ/kg. Here it is assumed that five additional wells can be drilled at well-pad B. The same output data is assumed for all the wells on pad B according to power plant design.

Well NWS-3 on pad C is currently reserved for brine re-injection, but pad C can readily accommodate additional brine re-injection wells. There is more than adequate area available in the immediate vicinity to well-pad C for a binary power plant, so the brine from the separator station will be transferred to the binary power plant on pad C and then re-injected to the injection wells on this pad.

4.2 Power plant technologies and costs

Generation of electricity using geothermal resources has been practised for a century, since its first use at the Lardarello geothermal field in Italy, in 1904. The steam Rankine cycle has been the conventional technology used for most worldwide geothermal power generation to date. The basic technology is analogous to the steam Rankine cycle used in thermal power plants except that the steam comes from the geothermal reservoir, rather than a boiler. Various technical enhancements to the condensing steam turbines have been implemented over the years to address the differences between geothermal and boiler-quality steam.

The most attractive geothermal fields for developers have been those with high resource temperatures and production fluid enthalpies. These fields can deliver at higher pressures and steam flash proportions in order to achieve more efficient operation of the condensing steam turbines, and hence lower electricity production costs. Condensing steam plants are typically used for resource temperatures in excess of 200°C.

For a low-enthalpy resource, a low operating pressure is needed to obtain a reasonable steam flash, equipment is larger and hence more expensive, and a significant proportion of the available energy in the production fluid is rejected in the separated brine. There are several experienced and competent providers around the world for steam-turbine geothermal power plants and component equipment. Turbine-generator unit capacities are typically in the 20-80 MWe range, but are offered from less than 5 MWe up to 110 MWe (SKM, 2005).

SUNA's brief included the preliminary investigation of a range of power plant capacities from 10 MWe to as much as 100 MWe. It was recognised that any options involving a large-scale development must necessarily be somewhat speculative until further geophysical fieldwork is completed and the indicated resource is confirmed by exploration drilling.

Economies of scale dictate that the largest possible power plant capacity will be preferred on a strictly economic basis. Other issues, including risk minimisation, may indicate a staged development using multiples of smaller unit capacity. These smaller units may be installed in sequence as knowledge of the resource grows and there is greater confidence in its capacity and longevity. Although sacrificing the major economies of scale, small capital and operating cost saving may be gained using multiple units installed within a common power house.

General site services and facilities required for power plant development include:

- Workshops and stores;
- Contractor and administration accommodation;
- Plant and construction services including potable water, compressed air, etc.,
- Transmission line facilities subject to capacity constraints.

4.3 Steam condensing with parallel binary ORC power plant

The binary organic Rankine cycle with a parallel steam condensing turbine (steam Rankine cycle) has been selected as the power plant system in this report. In this system, the two-phase fluid from wellheads goes to a separator station, separated steam is sent to a condensing steam turbine plant, and brine is transferred to the binary plant.

4.4 Separator station

Because the Mt. Sabalan field is a wet steam field, steam field separators are required. It is assumed that the separator station is located adjacent to the production well-pad to reduce pressure losses. Pressure losses between wellhead and separator, and between separator and power plant, imply an interface pressure of 3 bar-a. This assumes a relatively large pressure drop between wellhead and interface and the steam demand used in the calculation is therefore conservative.

Separators can be both vertical and horizontal. In previous designs of steam supply systems in many geothermal field developments throughout the world, the separators have been of the vertical centrifugal type, but recently the horizontal type has also been used. With some 30 years of experience behind it, the Weber-type bottom-outlet separator (Figure 4) has evolved into a highly efficient steam-field component. This design is capable of adapting to steam capacities of between 10 and 100 MWe capacity and, with appropriate attention to pressure control, will deliver separation efficiencies (measured as residual moisture in steam) of better than 99.9% (SKM, 2005).

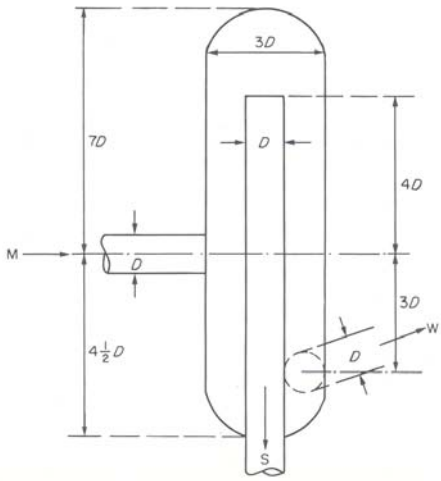

FIGURE 4: Schematic arrangement of Weber-type separator (Armstead, 1983)

We have assumed that a new geothermal development based on a wet steam resource will be operated as a base-load plant. Although this implies a constant steam demand, the steam-field and separator station require pressure control and a steam venting system will therefore be required. We propose

pressure control by means of steam venting to rock mufflers, using pressure-controlled vent valves. Pressure protection will be required by means of pressure relief valves, bursting discs, or both (SKM, 2005). The separator station includes level control valves, rupture discs, steam vent valves and emergency brine dump valves.

The characteristics of two-phase fluid are known. For calculations, pressure in the steam separator P_{sep}, needs to be known. This pressure depends on wellhead pressure and demand steam turbine pressure. Steam fraction in the separator (x_1) is:

$$x_1 = \frac{(h_1 - h_3)}{(h_2 - h_3)} \tag{1}$$

Steam mass flow ($\dot{m}_2$) is:

$$\dot{m}_2 = x_1 \dot{m}_{tot} \tag{2}$$

Brine mass flow ($\dot{m}_3$) is:

$$\dot{m}_3 = (1 - x_1) \dot{m}_{tot} \tag{3}$$

where $\dot{m}_{tot} = \dot{m}_1$ = Total mass flow from the production wells.

Mass conservation for the separator is shown in Figure 5.

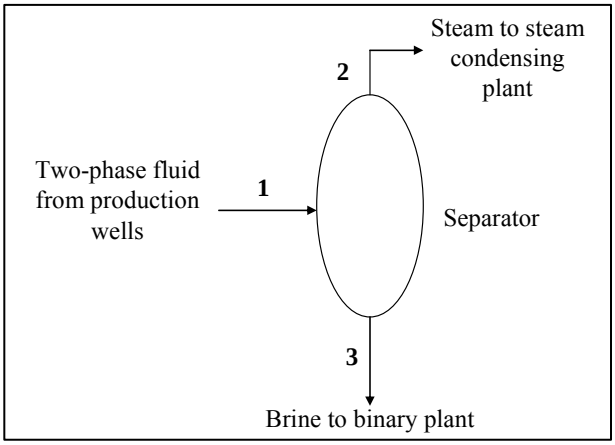

FIGURE 5: Mass conservation for a steam separator

4.5 Pipe sizing

Hydraulic analysis of the proposed steam piping system cannot be attempted in this early report. The steam, brine and condensate piping have been sized on a fluid velocity basis (SKM, 2005):

- The maximum steam velocity is 30 m/s;
- The maximum brine or condensate velocity is 1.5 m/s;
- An allowance of 10 m of 12´´ pipe per well has been made to connect each well on a well-pad to the two-phase header;
- An allowance of 50 m of 12´´ pipe has been made for the vent line at the pressure control stations.

Once a preferred option has been selected and the pipe routes confirmed, the pressure loss considerations may dictate that sections of the steam field system should be reviewed. This will have a minimal impact on the overall capital cost of the project and hence on the economic analysis.

5. POWER PLANT LOCATIONS AND STEAM AND BRINE PIPE SIZING DESIGN

The existing warehouse location and pad-C have been selected as the steam condensing plant and binary plant locations, respectively. The steam mass flow is:

$$\dot{m}_2 = \rho_s v_s (\frac{\pi D_s^{\ 2}}{4}) \tag{4}$$

where D_s = Inner diameter of the steam pipe;
ρ_s = Density of the steam;
v_s = Velocity of the steam.

Steam pressure drop Δp (bar-a) between well-pad B and the power plant is calculated as:

$$\Delta p = (\rho_s g \Delta z + h_L) 10^{-5} \tag{5}$$

with,

$$h_L = f \frac{L_s}{D_s} \frac{v^2}{2g} \tag{6}$$

and,

$$\left(\frac{1}{\sqrt{f}}\right) = -2\log\left[\frac{\varepsilon/D_s}{3.7} + \frac{2.51}{\mathrm{Re}\sqrt{f}}\right] \tag{7}$$

$$\mathrm{Re} = \rho_s v_s \frac{D_s}{\mu_s} \tag{8}$$

where Δz = Elevation difference between well-pad B and the power plant location;
h_L = Head loss;
f = Friction factor for turbulence flow;
ε = Pipe roughness;
Re = Reynolds number.

The same equations are used for the brine pipe sizing and pressure drop calculation from well-pad B to the binary plant at pad C by substituting brine parameters. Pipe calculations are performed by using the equations and DIN 2458 (St 37-2). Standard values are presented in Table 3.

TABLE 3: Pipe design results

Parameters	Steam pipe	Brine pipe
Length (m)	250	2200
Flow rate (kg/s)	44.64	255.4
Size (inch)	32	18
Thickness (mm)	6.3	4.5
Pressure drop (bar)	0.01	-19
Temperature drop (°C)	0.8	1.8
Insulation thickness (mm)	100	20
Length between supports (m)	19	14
Expansion loop length (m)	47	60

Related equations are presented in Appendix I.

6. STEAM CONDENSING PLANT

A typical process schematic is presented in Figure 6 for geothermal power generation. Conventional geothermal power plant development would require at least the following systems:

- Main steam inlet piping with control valves, emergency stop valves, steam strainer, etc.;
- Steam turbine/generator complete with lube oil and control systems, gland steam systems, turbine drains, etc.;
- Main condenser (direct contact) with non-condensable gas extraction systems;
- Circulating water system with cooling towers, pumps and control valves;
- Auxiliary cooling water system (and possibly a second clean water system);
- Plant services including heating, ventilation and air conditioning systems, compressed air, potable and processing water, fire fighting system, etc.;
- Turbine hall crane (may be extended tracks from an existing system);
- Electrical systems including excitation, switchgear, circuit breakers, step up transformers (from stator to grid voltage), plant bus with low and medium voltage reticulation system (for large motor loads) etc.;
- Emergency power supply, including battery banks and chargers.

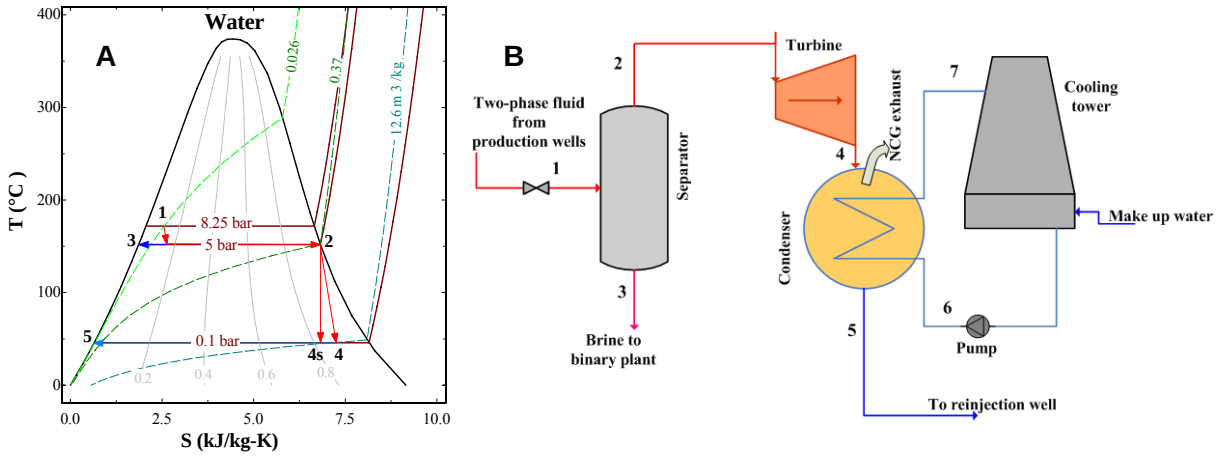

FIGURE 6: a) Steam condensing process; and b) system

6.1 Steam turbine

Steam flowing from the separators enters the steam turbine. The steam is supplied to the turbine rotor via nozzles in a tangential direction at higher velocity. The turbine rotor is subjected to an axial thrust as a result of pressure drops across the moving blades and changes in rotational momentum of the steam between the entrance and exit, and then passed through the rotor shaft as useful power output of the turbine. The capacity of the turbine is a fundamental factor in the design of a geothermal power plant. Some factors that influence the selection are available steam, thermodynamic and chemical characteristics of the steam, type of turbine, effects of natural decline in flow rate and pressure of the wells, decrease or increase of the non-condensable gases, and financial factors at present and in the future.

The turbine material is carefully selected for resistance to corrosion due to the presence of hydrogen sulphide and salt (chloride), and scale components such as silica oxide, aluminium oxide, and sulphur oxide. The blade material is also resistive to erosion due to the presence of condensate or brine and

solid particles such as corrosion products. However, the best way to avoid the appearance of corrosion and erosion is to keep steam impurities out of the turbine (Mitsubishi, 1993).

It is assumed that turbine efficiency is 85%. Since dry expansion is more efficient than wet expansion, it is proposed that high efficiency is maintained by installing an inter-stage drain catcher. Reducing the wetness of the steam also decreases the effect of water erosion.

The output power of the turbine is calculated as:

$$\dot{W}_{Tur} = \dot{m}_2 (h_2 - h_4)\eta_s \tag{9}$$

where $\dot{m}_2$ = Steam mass flow;
η_s = Isentropic efficiency of the turbine;
h_2 and h_4 = Inlet and outlet enthalpies, respectively.

6.2 Condenser

The primary purpose of the condenser is to condense the exhaust steam from the turbine. The circulating-water system supplies cooling water to the turbine condensers and thus acts as the unit by which heat is rejected from the steam cycle to the environment. The circulating system is efficient but also has to conform to thermal-discharge regulations. Its performance is vital to the efficiency of the power plant itself because a condenser operating at the lowest temperature possible results in maximum turbine work and cycle efficiency and minimum heat rejection.

The heat transfer process is governed by different temperatures and a mass transfer process of exhaust steam and cooling water. The condensation process occurs when the latent heat of the steam is absorbed as sensible heat by cold water. In order to generate maximum useful energy in the turbine, the condenser pressure stays in vacuum conditions. Theoretically, the more vacuum created, the more useful energy is gained. The condenser vacuum attainable in practice is, however, restricted by the specific volume of steam, the type of condenser and evacuation process selected, and the amount of non-condensable gas present in the steam. The typical condensate temperature attained in practice is 45-50°C, corresponding to a condenser pressure of 0.0959-0.1234 bar-a (El-Wakil, 1984).

Condenser evacuation equipment not only evacuates the non-condensable gases but also some of the associated water vapour. This reduces condenser evacuation efficiency, and further limits the attainable vacuum.

Figure 7 shows the temperature distribution in the condenser. The circulating-water inlet temperature should be sufficiently lower than the steam-saturation temperature to result in reasonable values of ΔT_o. It is usually recommended that ΔT_i should be between about 11 and 17°C and that ΔT_o, the TTD, should not be less than 2.8°C. The enthalpy drop and turbine work per unit pressure drop are much greater at the low-pressure end than at the high-pressure end of a turbine (El-Wakil, 1984).

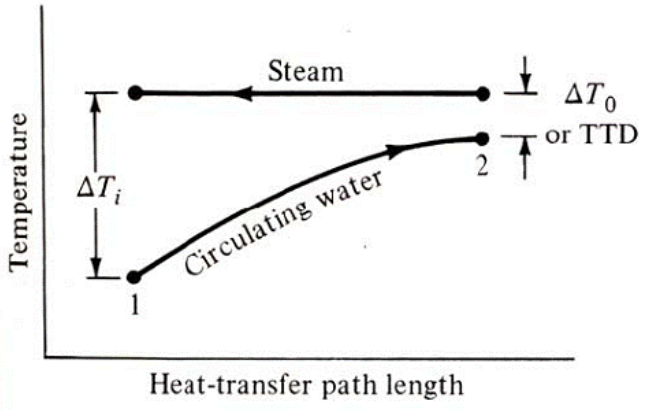

FIGURE 7: Condenser temperature distribution

A condenser with a low back pressure of only a few pa, increases the work of the turbine, increases plant efficiency, and reduces the steam flow for a given plant output. A condenser is a major component in a power plant and a very important piece of equipment. There are two types of condensers, direct contact and surface condensers. The most common type used in power plants is surface condensers.

The heat transfer over the condenser is calculated as:

$$Q = \dot{m}_2(h_4 - h_5) \tag{10}$$

where h_4 and h_5 = Enthalpies into and out of the condenser, respectively.

The circulating water flow and the pressure drop through the condenser are determined according to the following equations, the water mass flow rate is:

$$\dot{m}_w = \frac{Q}{c_p(T_2 - T_1)} \tag{11}$$

where c_p = Specific heat of the water; and
T_1 and T_2 = Inlet and exit temperatures, respectively.

The pressure drop is given in terms of head, H, which is related to the pressure loss, Δp by:

$$\Delta p = \rho H \frac{g}{g_c} \tag{12}$$

where ρ = Density;
g = Gravitational constant;
g_c = Conversion factor, 1.0 N m/(kg s^2).

Water inlet velocities in condenser tubes are usually limited to a maximum of 2.5 m/s to minimize erosion, and a minimum of 1.5-1.8 m/s for good heat transfer. Values between 2.1 and 2.5 m/s are most common (El-Wakil, 1984).

6.3 Gas removal system

Geothermal steam contains non-condensable gases in large amounts compared with that of conventional thermal power plants. It is well known that gases in geothermal steam influence the design of the main part of the power plant equipment such as the turbine, condenser, cooling tower, and gas extraction system.

This is caused not only by corrosion problems but also by the high volume of gases occupied in the turbine and condenser. As a rule of thumb, if the amount of gases is more than 10%, it is more economic to expand the steam in the back pressure turbine; otherwise an expensive gas extraction system has to be installed.

In steam and other vapour cycles, it is important to remove the non-condensable gases that otherwise accumulate in the system. The presence of non-condensable gases in large quantities has undesirable effects on equipment operation for several reasons:

- It raises the total pressure of the system as the total pressure is the sum of the partial pressures of the constituents. An increase in condenser pressure makes plant efficiency lower.

- It blankets the heat-transfer surfaces such as the outside surface of the condenser tube and makes the condenser less effective.
- The presence of some non-condensable gases results in various chemical activities.

Some geothermal power plants use steam-jet ejectors to extract non-condensable gases. For high performance, non-condensable gas extraction will be achieved by using an electrically driven vacuum pump. The power of the vacuum pump is calculated by the following equation (Siregar, 2004):

$$P_{Vpump} = \left(\frac{\gamma}{\gamma - 1}\right) \frac{m_g R_u T_{cond}}{\eta_{Vpump} M_{gas}} \left[\left(\frac{P_{atm}}{P_{cond}}\right)^{\left(1-\frac{1}{\gamma}\right)} - 1\right] \tag{13}$$

where P_{Vpump} = Power of the pump (kW);
γ = $C_{p,gas} / C_{v,gas}$
m_g = Mass flow rate of the gas (kg/s);
R_u = 8.314 kJ/(kmol K), the universal gas constant;
T_{cond} = Temperature of the condensate (K);
η_{Vpump} = Efficiency of the pump;
M_{gas} = Molar mass of the gas;
P_{atm} and P_{cond} = Atmospheric and condenser pressures (bar-a), respectively.

It is possible to use the combination of a steam ejector and a liquid ring vacuum pump as a gas exhaust system when the motor driving the vacuum pump needs more power.

6.4 Cooling system

In general, geothermal resources are located in remote areas, and often in mountainous areas. Cold groundwater is not always found in enough volume to be economical. This is why geothermal power plants are usually equipped with cooling towers, either wet or dry.

The function of a cooling tower is to decrease temperature from the inlet to the outlet of the tower based on the temperature difference between the warm water inlet and ambient temperature. An efficient cooling tower will give a high temperature difference between the inlet and outlet water with a low temperature difference between the inlet water and ambient temperature.

6.4.1 Wet cooling tower

A cooling tower is an evaporative heat transfer device in which atmospheric air cools warm water, with direct contact between the water and the air, by evaporating part of the water. Wet cooling towers have a hot water distribution system that showers or sprays the water evenly over a latticework of closely set horizontal slats or bars called fill or packing. The fill thoroughly mixes the falling water with air moving through the fill as the water splashes down from one fill level to the next.

Outside air enters the tower via louvers in the form of horizontal slats on the side of the tower. The slats usually slope downward to keep the water in. The intimate mix between water and air enhances heat and mass transfer (evaporation) which cools the water. The cold water is then collected in a concrete basin at the bottom of the tower where it is pumped back to the condenser. The now hot, moist air leaves the tower at the top.

6.4.2 Mechanical-draft cooling tower

In mechanical-draft cooling towers, the air is moved by one or more mechanically driven fans. The majority of mechanical-draft cooling towers for utility application are, therefore, of the induced-draft type. With this type, air enters the sides of the tower through large openings at low velocity and passes through the fill. The fan is located at the top of the tower, where the hot, humid air exhausts to the atmosphere. The fans are usually multi-bladed and large, ranging from 20 to 33 ft (6-10 m) in diameter. They are driven by electric motors, as large as 250 hp, at relatively low speeds through reduction gearing. The fans used are of the propeller type, which results in large volumetric flow rates at relatively low static pressure. They have adjustable-pitch blades for minimum power consumption, depending on system head load and climatic conditions.

6.4.3 Additional (makeup) water

In the cooling-water system, some water will be lost due to evaporation, drift and bleeding or blow down. Makeup water required by a cooling tower is the sum of that which would compensate for the water loss. This water, in addition to compensating for evaporation and drift, keeps the concentration of salts and other impurities down. Otherwise, these concentrations would continuously build up as the water continues to evaporate. The evaporation loss rate is 1-1.5% of the total circulating water flow rate. Blow down is normally 20% of evaporation loss but sometimes the value is similar to evaporation loss, depending upon the content of chemicals and various minerals, and the size of the plant. Water droplet size will vary with exchanger type, condition of the media, air velocity through the unit, and other factors. The drift loss is perhaps 0.03% of the total circulating water flow rate. A large quantity of drift cannot be tolerated, as it can cause water and ice deposition problems at and near the plant area.

6.4.4 Wet cooling tower calculations

To find and calculate the energy balance, mass balance, and power consumption for the fan at the cooling tower, the following parameters must be known (El-Wakil, 1984):

- *Dry-bulb temperature* (T_{db}) is the temperature of the air as commonly measured and used.
- *Wet-bulb temperature* (T_{wb}) is the temperature of the air measured psychrometrically (Perry, 1950); if the air is saturated, i.e. φ = 100%, the wet-bulb temperature equals the dry-bulb temperature.
- *Approach* is the difference between the cold-water temperature and the wet-bulb temperature of the outside air.
- *Range* is the difference between the hot-water temperature and the cold-water temperature.
- *Relative humidity* (φ) is the partial pressure of water vapour in the air, (P_v), divided by the partial pressure of water vapour that would saturate the air at its temperature (P_{sat}), or:

$$\varphi = \frac{P_v}{P_{sat}} \tag{14}$$

- *Humidity ratio* is the air per unit mass of dry air, or:

$$\omega = \frac{53.3P_v}{85.7P_a} = \frac{0.622P_v}{P - P_v} \tag{15}$$

where 53.3 and 85.7 are the gas constants for dry air and water, respectively.

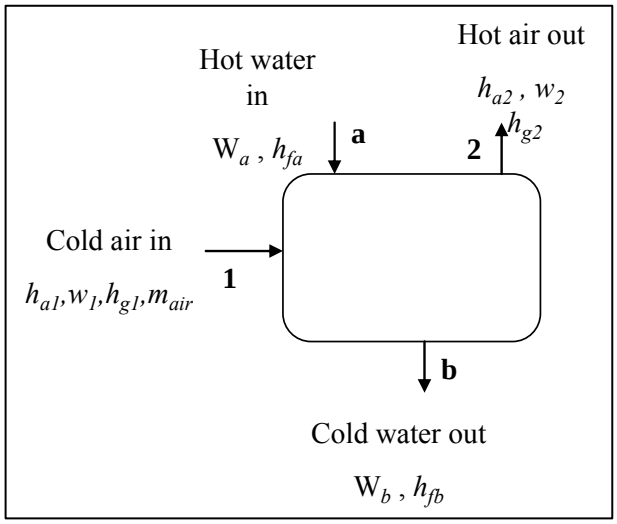

FIGURE 8 : Energy balance in a cooling tower

6.4.5 Energy balance

The energy balance between hot water and cold air entered, cold water and hot air exiting the cooling tower is shown in Figure 8. Changes in potential and kinetic energies and heat transfer are all negligible. No mechanical work is done. Thus, only enthalpies of the three fluids appear. The subscripts 1 and 2 refer to air inlet and exit, the subscripts a and b refer to circulating water inlet and exit, respectively. To define the energy balance, the following variables are used:

For the water:

W_a = Mass of hot water entering the cooling tower (kg);

h_{fa} = Enthalpy for the liquid entering the cooling tower (J/kg);

W_b = Mass of cold water exiting the cooling tower (kg);

h_{fb} = Enthalpy for the liquid exiting the cooling tower (J/kg).

For the air:

h_{a1} = Enthalpy for the cold dry air (at 20°C) (J/kg) (from psychrometric chart, Perry, 1950);

ω_1 = Humidity ratio for the cold air;

h_{g1} = Enthalpy of the cold water vapour (J/kg) (from steam table);

h_{a2} = Enthalpy of the hot dry air (40°C) (J/kg) (from psychrometric chart, Perry, 1950);

ω_2 = Humidity ratio for the hot air;

h_{g2} = Enthalpy of the hot water vapour (J/kg) (from steam table).

Following psychrometric practice, the equation for a unit mass of dry air can hence be written as:

$$h_{a1} + \omega_1 h_{g1} + W_a h_{fa} = h_{a2} + \omega_2 h_{g2} + W_b h_{fb} \tag{16}$$

6.4.6 Mass balance

The dry air goes through the tower unchanged. The circulating water loses mass by evaporation. The water vapour in the air gains mass due to the evaporated water. Thus, based on a unit mass of dry air:

$$\omega_2 - \omega_1 = W_a - W_b \tag{17}$$

This results in the energy balance equation:

$$\omega_1 h_{g1} + W_a h_{fa} = c_p (T_2 - T_1) + \omega_2 h_{g2} + \left(W_a - (\omega_2 - \omega_1)\right) h_{fb} \tag{18}$$

where c_p = Specific heat of air; and

T_2-T_1 = Temperature difference between inlet and exit air temperature through cooling tower.

6.4.7 Power of fan

To calculate the power of the fan P_{fan} (W) at the cooling tower, the equation is:

$$P_{fan} = \frac{\dot{V}_{air}\,\Delta p}{\eta_{fan}} \tag{19}$$

and,

$$\dot{V}_{air} = \frac{\dot{m}_{air}}{\rho_{air,out}} \tag{20}$$

Thus,

$$P_{motor,fan} = \frac{P_{fan}}{\eta_{motor,fan}} \tag{21}$$

where Δp = Pressure drop (pa);
$\dot{V}_{air}$ = Volume flowrate of air (m^3/s);
$\dot{m}_{air}$ = Mass flow of the air (kg/s);
$\rho_{air,out}$ = Density of the air out of the cooling tower (kg/m^3); and
η_{fan} and $\eta_{motor\,fan}$ = Efficiency of the fan and the motor of the fan, respectively.

6.4.8 Power of pump

The following equations are used to calculate the power of the pump:

$$P_{pump} = \frac{\dot{V}_{water}\,\Delta p}{\eta_{pump}} \tag{22}$$

$$\dot{V}_{water} = \frac{\dot{m}_{water}}{\rho_{water}} \tag{23}$$

and;

$$P_{motor,pump} = \frac{P_{pump}}{\eta_{motor,pump}} \tag{24}$$

where Δp = Pressure drop (pa);
$\dot{V}_{air}$ = Volume flowrate of water (m^3/s);
$\dot{m}_{air}$ = Mass flowrate of the water (kg/s);
$\rho_{air,out}$ = Density of the water (kg/m^3); and
H_{pump} and $\eta_{motor\,pump}$ = Efficiency of the pump and the motor of the pump.

6.5 Steam turbine plant capital costs

Steam turbine costs have been assembled from a range of relevant geothermal projects around the world. There is a strong inverse relationship between capacity and specific capital cost. Capital costs presented in Table 4 below include all components of a standard steam turbine plant as well as engineering, procurement, contract management, plant installation and commissioning.

TABLE 4: Capital costs for a range of conventional steam turbine power plant capacities (SKM, 2005)

Plant generation capacity (MWe)	**10**	**20**	**20**	**40**	**40**	**80**	**100**
Plant configuration	1×10	2×10	1×20	2×20	1×40	2×40	2×50
Capital cost, installed (MUS$)	32	54	50	86	80	136	158
Specific capital cost (US$/KWe)	3160	2690	2520	2140	2000	1700	1580

Table notes: 1. Capital cost data factored from current bidding using 0.67 exponents;
2. 15% cost saving for two units of similar capacity on same site;
3. 20% cost penalty imposed for anticipated low pressure steam.

Table 5 lists all parameters for the range of development scenarios analyzed, assuming the economy of scale in capital and O&M costs (operations and maintenance) as well as the sensitivity of productivity decline to plant capacity (Sanyal, 2005).

TABLE 5: Development scenarios cost analyzed (Sanyal, 2005)

Plant capacity (MWe)	**Unit capital cost (US$/kW)**	**Total capital cost (MUS$)**	**Unit O&M cost (US¢/kWh)**	**Initial harmonic decline rate (%)**	**No. of initial product. wells**	**Years before make-up well**
5	2500	12.5	2	0.2	2	>30
10	2463	24.6	1.98	0.6	3	>30
20	2390	47.8	1.93	1.5	5	9
30	2319	69.6	1.88	2.6	7	2
50	2184	109.2	1.79	5	11	0
75	2025	152	1.68	8.3	17	0
100	1880	188	1.58	11.8	22	0
125	1744	218	1.48	15.4	28	0
150	1618	242.7	1.39	19.2	33	0

Based on Tables 4 and 5, the cost in US$ for steam turbine plants in this report can be estimated as:

$$C_{plant} = 2500\dot{W}_{plant} \tag{25}$$

7. ORC BINARY PLANT

An organic Rankine cycle (ORC) power plant, which is also referred to as a ‘binary cycle’ plant, makes use of a ‘working’ or ‘motive’ fluid with a lower boiling point than steam. The particular fluid is selected based on the comparison of heat source temperature and motive fluid properties. Most existing geothermal ORC plants use low boiling point hydrocarbons – iso-pentane is most common, although there are also plants using iso-butane. It is also possible to use refrigerants, other organic compounds or a mixture of hydrocarbons as the working fluid, although this is less common in practice. In most geothermal ORC plants using hot water as the heat source fluid, the supply temperature is in the 140-200°C range, although there are several installed plants using cooler fluids down to 100°C. A heat source temperature of around 90°C is generally considered to be the economic minimum for power generation using ORC technology.

The first geothermal ORC plant was built in Russia in the 1960s; however extensive commercial application of the technology did not begin until the 1980s. There are now dozens of geothermal ORC power plants in operation around the world, ranging in output from 200 kW to 125 MW. ORC technology is also used for power generation from waste heat, and for small-scale, gas-fired remote power generation. Individual unit sizes are typically in the range from 250 kW to 10 MW, although a single 65 MW turbine operated at the US DOE's Heber binary demonstration plant for several years in the mid 1980s. Ormat International dominates the ORC power plant market. Other current or previous technology providers include Turboden, Bibb & Associates (formerly The Ben Holt Company) and Barber Nichols Engineering (SKM, 2005).

7.1 Process description

The working fluid operates in a contained, closed-loop cycle (Figure 9a) and is completely segregated from the heat source fluid. There are a number of possible variants of the cycle, in terms of heat exchange configuration, turbine configuration, etc., which may be selected as appropriate to the temperature and physical state(s) of heat source fluid. A simplified schematic diagram of a typical ORC power plant that has been selected in this report is also presented in Figure 9b.

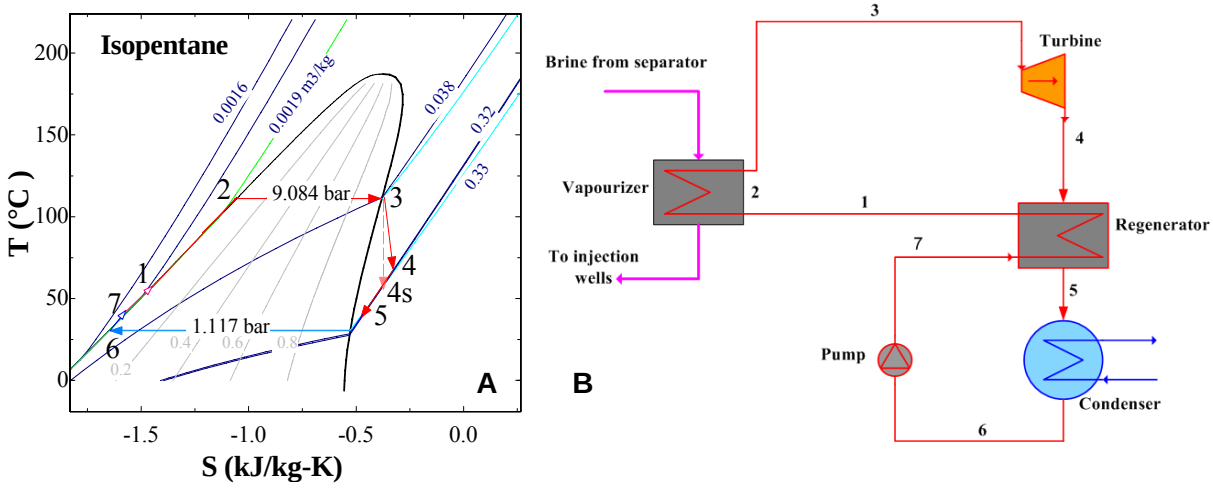

FIGURE 9: Binary ORC system and process; a) the closed-loop cycle for the working fluid; b) schematic diagram of a typical ORC power plant

The working fluid absorbs heat from a heat source, in this case the hot geothermal fluid, via one or more shell and tube heat exchangers. This heat causes the working fluid to evaporate; producing the high-pressure vapour that is then expanded through a turbine-generator. The low-pressure turbine exhaust vapour is then led to the regenerator. In this exchanger, residual sensible heat in the low-pressure turbine exhaust stream is used for initial preheating of the cold liquid from the motive fluid pump, thus increasing cycle efficiency. The cooled regenerator exhaust vapour is then condensed, using either air-cooled heat exchangers ('fin-fan exchangers'), or a water-cooled, shell-and-tube condenser. Air cooling is appropriate in locations with limited water supplies, although the motive fluid outlet temperature is then limited by the prevailing ambient dry-bulb, rather than wet-bulb, temperature. From the condenser, the liquid working fluid is pumped to a high pressure and returned to the regenerator to close the cycle.

7.2 Heat exchangers

There are three heat exchangers in the binary cycle. In the vaporizer, heat is transferred from geothermal brine coming from the separator into isopentane to vaporize it. Heat is transferred through

the regenerator to preheat the cold liquid coming from the pump. These two heat exchangers are shell and tube type. The air-cooled condenser is a fin-fan type heat exchanger in which low-temperature vapour coming from regenerator is condensed by heat transfer to ambient air which is blown via the fans to the condenser.

7.2.1 Vaporizer

This heat exchanger is a device that facilitates heat transfer from geothermal brine to binary working fluid (iso-pentane). The heat exchange process between geothermal brine as hot fluid and iso-pentane as cold stream is shown in Figure 10. The point at which the two curves come closest is called the pinch point, and the corresponding temperature is called the pinch temperature. The pinch point divides the process into two thermodynamically separated regions. The pinch point is shown by arrows in Figure 10. The pinch temperature is the lowest temperature difference between the hot and cold fluids during the heat exchange. Below the pinch, there is a heat surplus and only utility cooling is required. Any utility heating supplied to the process below the pinch temperature cannot be absorbed and will be rejected by the process to the cooling utility, increasing the amount of cooling utility required. The area above the pinch requires only utility heating and no utility cooling. Any utility cooling above the pinch temperature has to be made up by additional utility heating (Mineral Processing Research Institute, 2001).

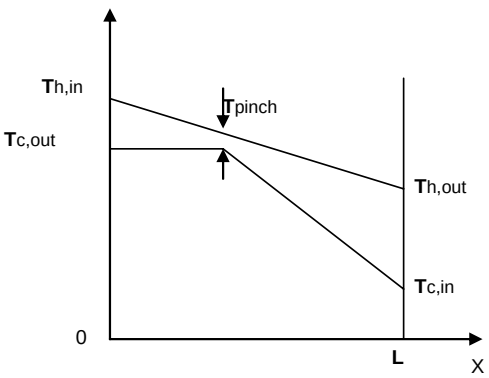

FIGURE 10: Heat exchange process in vaporizer

The following energy balance equations are used for heat exchangers, in which the vaporizer is treated in two steps:

$$\dot{Q} = \dot{m}_{H,in}\left(h_{H,in} - h_{H,out}\right) = \dot{m}_{C}\left(h_{C,out} - h_{C,in}\right) \tag{26}$$

$$\dot{Q} = (\dot{m}c_p)_H\left(T_{H,in} - T_{H,out}\right) = (\dot{m}c_p)_C\left(T_{C,out} - T_{C,in}\right) \tag{27}$$

$$\dot{Q} = UA \times LMTD \tag{28}$$

where U = Overall heat transfer coefficient (°C/m^2);
A = Heat transferring area (m^2); and
$LMTD$ = Logarithmic Mean Temperature Difference (°C), which is abbreviated as LMTD and calculated as:

$$LMTD = \frac{\left(T_{hot,in} - T_{cold,out}\right) - \left(T_{hot,out} - T_{cold.in}\right)}{\ln\left(\dfrac{T_{hot,in} - T_{cold,out}}{T_{hot,out} - T_{cold,in}}\right)} \tag{29}$$

Figure 11 presents the amorphous silica saturation curve for fluid from well NWS4. The curve shows that brine from the separator is not saturated with respect to amorphous silica until it reaches a temperature of about 100°C. This result indicates that silica deposition will start when the brine cools down below 100°C. It means that the temperature of vaporizer outlet brine to the re-injection well should be higher than 100°C.

7.3 Binary plant costs

Based on historical prices, the capital cost of an air-cooled ORC power plant fed by hot water should be in the range US$1250-1800 per kW (net), for heat source temperatures in the 100-200°C range and for a 3–30 MWe multi-unit development. This cost would cover an EPC power plant, excluding the geothermal fluid supply and return reticulation systems. The historical prices vary quite widely (US$950 to over 2,000 per kW) and the plants in question have a wide range of operating conditions, making it difficult to draw firm correlations for the effects of project scale and resource temperature, although the specific capital cost ($/kW) will increase as resource temperature decreases. The available temperature range between heat source and sink temperatures decreases and, as a result, the required surface area for heat exchangers and condenser must increase. The lower grade of heat supply also affects the operating conditions in the binary cycle, pushing equipment costs up (SKM, 2005).

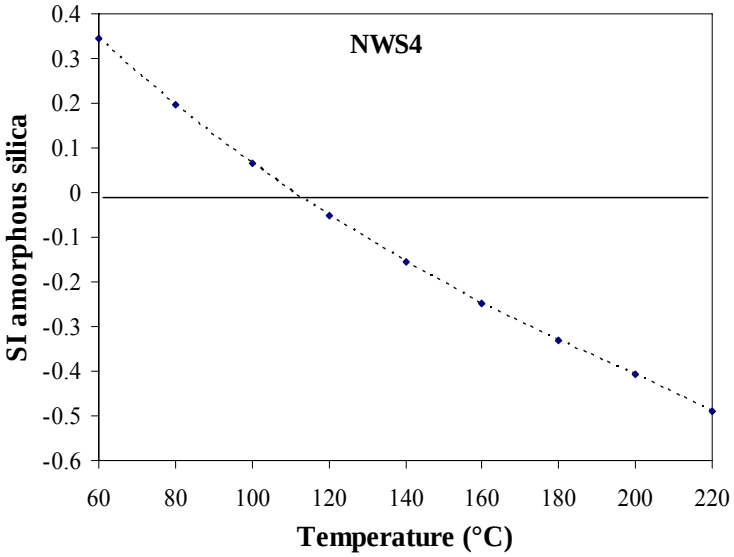

FIGURE 11: Calculated state of amorphouse silica saturation of NWS4 fluid upon adiabatic boiling

The estimated purchased equipment costs (PEC) are obtained from the following equations. Values are adapted from Valero et al. (1996) for an ORC cycle. All costs are in US$:

$$PEC_{Pump} = \left(\frac{C_{11}\dot{m}_{Iso}}{C_{12} - \eta_P} \right) \left(\frac{P_7}{P_6} \right) \ln\left(\frac{P_7}{P_6} \right) \tag{30}$$

$C_{11} = 25$ $/(kg/s); and $C_{12} = 0.9$

$$PEC_{Turb} = \left(\frac{C_{31}\dot{m}_{Iso}}{C_{32} - \eta_{Turb}} \right) ln\left(\frac{P_3}{P_4} \right) \left(1 + Exp(C_{33}T_1 - C_{34}) \right) \tag{31}$$

$C_{31} = 2000$ $/(kg/s); $C_{32} = 0.92$; $C_{33} = 0.05$ K^{-1}; and $C_{34} = 50$

$$PEC_{HeatExchangers} = C_{41} A_{HX}^{0.6} \tag{32}$$

$C_{41} = 5000$ $/m^2

$$Cost_{piping} = 0.1(PEC_{vap} + PEC_{con} + PEC_{reg} + PEC_{tur} + PEC_{pump}) \tag{33}$$

$$COST_{tot} = PEC_{vap} + PEC_{con} + PEC_{reg} + PEC_{tur} + PEC_{pump} + Cost_{piping} \tag{34}$$

$$C_{net} = \frac{COST_{tot}}{\dot{W}_{net}} \tag{35}$$

8. DESIGN CALCULATIONS

The Engineering Equations Solver (EES) program was used to perform the calculations.

8.1 Power output of turbine generator in steam condensing plant

A fundamental factor in the design of a geothermal power plant is the capacity of the turbine. The steam flowing from the separator and entering the turbine is 44 kg/s. Steam enters the turbine at approximately 151°C and at 5 bar-a. The steam expands in the turbine, converting the thermal and pressure energy of the steam to mechanical energy, which is converted to electrical energy in the generator. The steam exhaust from the turbine is at 0.1 bar pressure and 46°C saturation temperature and is condensed in the surface condenser. From Equation 9 the power output of the turbine generator is calculated to be *19 MWe*, but the value of the power output is actually less due to the power required for plant operation (pumps, cooling tower fan and so on).

8.2 Power required for plant operation in a steam condensing plant

Condenser. The temperature of exhaust steam from the turbine is 46°C. The steam flows through the condenser where it is condensed by the cold water passing through the condenser. The temperature of the cold water entering the condenser is 30°C. It is heated in the condenser. The rejected water takes heat from the condenser. The hot water is cooled again in the cooling tower. Mass flow of the cold water is calculated, using Equation 11, to be 1719 kg/s. Equation 24 is used to calculate the power requirement of the cooling water circulation pump, giving: *347 kW*.

The NCGs are continuously removed from the condenser by ejectors or vacuum pumps. Using Equation 13 to calculate the power required for the vacuum pump gives: *330.8 kW*.

Cooling tower, as is common in geothermal plants, a cooling tower of an induced draft type will be used. The calculation of the cooling tower involves energy and mass balance.

The hot water entering the cooling tower is cooled through heat exchange with the cold air inside the cooling tower. The temperature of the water after cooling is 30°C. The cold air temperature inside the cooling tower is 20°C, which is the same as the wet-bulb temperature (T_{wb}). The temperature difference between the steam entering the condenser and the hot water leaving the condenser is 3°C. The temperature difference between the hot water temperature entering the cooling tower and the hot air temperature exiting the cooling tower is 7°C. The approach is 5°C. From energy and mass balance calculations the power of the cooling tower fan is found to be *242 kW*. The additional (makeup) water needed to replace water loss through evaporation, drift and blow down is 36 kg/s. The water is pumped from a nearby river to the cooling tower. The exhaust steam from the turbine is condensed through the cooling process in the condenser. The condensate from the condenser will be retransferred to the injection wells.

8.3 Output of the steam condensing plant

The output of the power plant is found by deducting the power required for plant operation from the power of the generator, or:

$$P_{powerplant} = P_{turbine} - (P_{motor,Vpump} + P_{motor,pump} + P_{motor,fan}) \quad (36)$$

Calculations based on this equation give the power plant output as *18.011 MWe*.

8.4 Power output of the turbine generator in an ORC binary plant

The brine flowing from the separator is 255 kg/s. This flow is fed equally to three identical binary units. Therefore, each unit receives 85 kg/s mass flow rate at approximately 150°C. This flow rate enters into the vaporizer and vaporizes 52.6 kg/s of isopentane, where the brine is cooled to 90°C. The working fluid enters the turbine at approximately 111°C and 9.08 bar-a. It expands in the turbine, converting the thermal and pressure energy of the vapour to mechanical energy, which is converted to electrical energy in the generator. The working fluid exhaust from the turbine is at 1.15 bar pressure and 64.8°C. From Equation 9 the power output of each turbine generator is calculated to be *3.2 MWe,* but the value of the power output is actually less due to the power required for plant operation (pumps, condenser fan and so on).

The brine leaving the vaporizer is directed to the re-injection wells where it is re-injected back into the ground.

8.5 Power required for plant operation in a binary plant

Condenser fan and motive working fluid pump. The temperature of the exhaust fluid from the regenerator is 36.6°C. It is exhausted to an air-cooled condenser where it is condensed to a temperature of 30.7°C. Approximately 1589 m^3/s air at an ambient temperature of 20°C is required to absorb the heat yielded by the working fluid. This raises the air temperature to 30°C. The working fluid is pumped to the regenerator to complete the Rankine cycle. Equation 24 is used to calculate the power requirement of the motive working fluid pump, and it is *135 kW*.

Using Equation 19 to calculate the power required for the condenser fans gives *353 kW*.

8.6 Output of the binary plant

The output of the power plant is found by deducting the power required for plant operation from the power of the generator, or:

$$P_{Binaryplant} = P_{turbine} - (P_{motor,pump} + P_{motor,fan}) \tag{37}$$

Calculations based on this equation give the power plant output as 2.7 MWe. Therefore, the total output of the 3 binary units is *8.2 MWe.*

8.7 Total output of power plant

The net power outputs from steam condensing and binary Rankine cycles are 18 and 8.2 MWe, respectively. *Hence, the total net power output becomes 26.2 MWe.*

8.8 Total cost estimate for power plant

Using Equation 25 to calculate the estimated cost of a steam condensing plant gives approximately 45 MUS$. Equations 30 to 35 are used to calculate the estimated cost of a binary plant, and it is approximately 11.2 MUS$ for all three units. Therefore, the total cost of the power plant is estimated at about *56.2 MUS$.* The net cost is found using Equation 35, and it gives *2150 US$/kW*.

9. OPTMIZATION OF THE POWER PLANT OUTPUT

The steam condensing cycle and the binary cycle have been modelled separately by the EES (Engineering Equation Solver) program (see Appendix II). These models can be used to calculate the output of the power plant for various values of pressure in the steam separator, pressure in the condenser, different temperatures at the cold end of the vaporizer and the pinch temperature of regenerator. It will help when choosing the turbine size, the inlet pressure and the exhaust pressure of the turbine and design values for other power plant equipment.

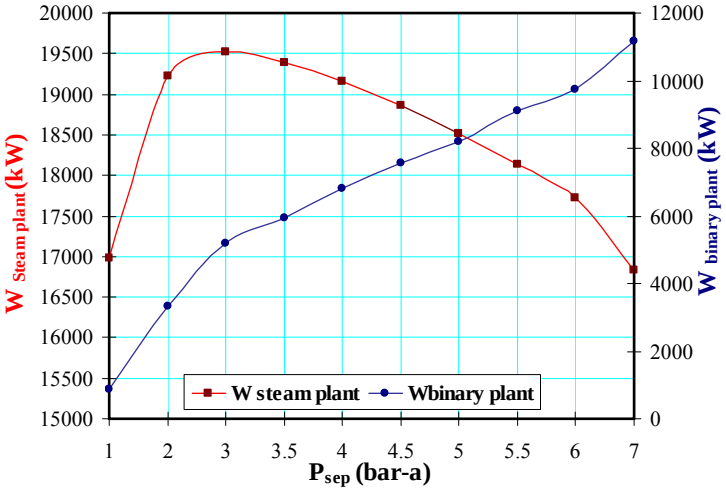

FIGURE 12: Separator pressure vs. power output of steam and binary plants

9.1 Optimum pressure of separator

The optimum pressure of the steam separator is defined as the pressure at which the output from the power plant is maximized. To find this optimum pressure of the separator, the pressure in the condenser is kept constant and the output of the power plant is calculated for different pressures in the separator, for example at 1 to 7 bar-a. The results of these calculations are shown in Figures 12 -14. In Figure 12 the output of the steam plant and binary plant is plotted vs. separator pressure. From the figure the optimum separator pressure for the steam plant is 3 bar-a but the optimum total output and cost for steam and binary plants is obtained when the separator pressure is 5 bar-a (Figures 13 and 14), where total output power and cost are 26.2 MWe and 56.2 mUS$, respectively.

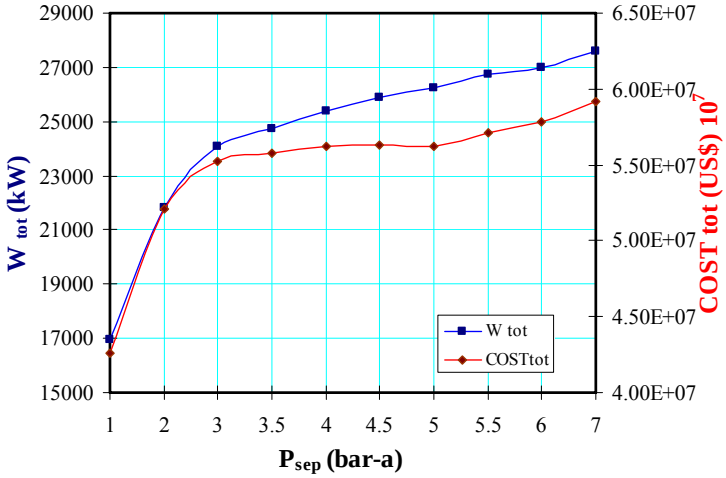

FIGURE 13: Total power output and total cost vs. separator pressure

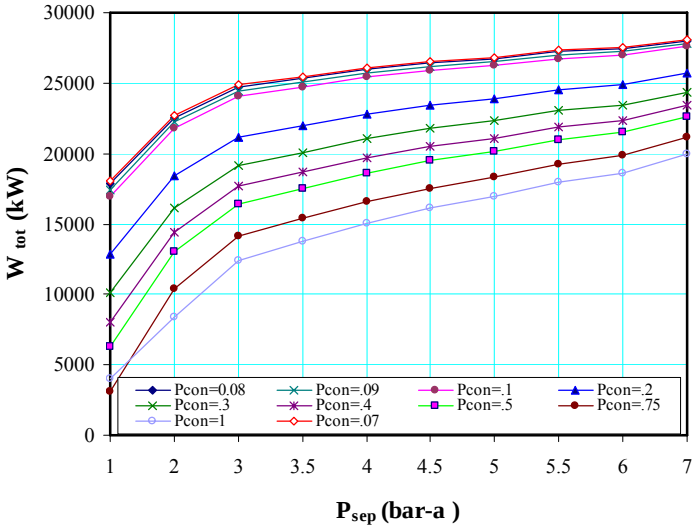

FIGURE 14: Total power output vs. separator pressure with different condenser pressure

9.2 Optimum pressure of condenser

The optimum pressure of the condenser, i.e. the pressure in the condenser at which the output from

the power plant is maximized, is calculated in the same way as the optimum pressure in the separator.

The output from the power plant is calculated for different pressures in the condenser while the pressure in the steam separator is kept constant. The results of these calculations are shown in Figure 14 where the output of the plant is plotted vs. pressure in the condenser for different pressures in the separator. This plot shows that the highest output is obtained when the condenser pressure is 0.07 bar-a, but Figure 15 shows that turbine outlet steam dryness is very low when condenser pressure is less than 0.1 bar-a. As can be seen in Figure 15, the steam dryness for turbine outlet is 86% when condenser pressure is 0.1 bar-a. Therefore, the optimum condenser pressure is 0.1 bar-a when the separator is operating in 5 bar-a. Total output from the steam plant in these conditions is 18 MWe.

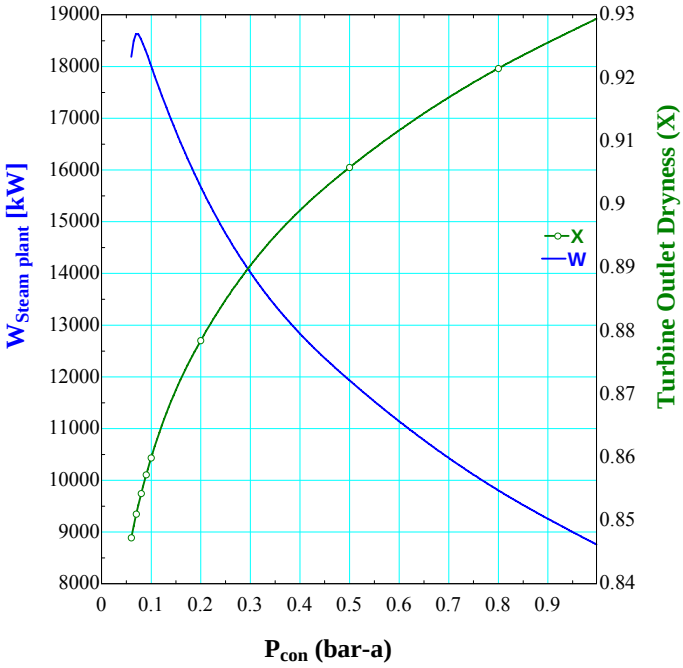

FIGURE 15: Steam plant output and steam dryness vs. condenser pressure

9.3 Optimum temperature of the brine in cold end of the vaporizer

The optimum temperature of the brine outlet of the vaporizer is defined as the temperature at which the output from the power plant is maximized. To find this optimum temperature, the output of the power plants is calculated for different temperatures in the cold end of the vaporizer, for example at 40 to 140°C. The results of these calculations are shown in Figure 16. It can be seen from the figure that the highest power output is at 75°C but brine temperature is limited by silica saturation temperature which was calculated by the WATCH program (see Figure 11). Therefore, the temperature, of 90°C was selected for vaporizer outlet brine.

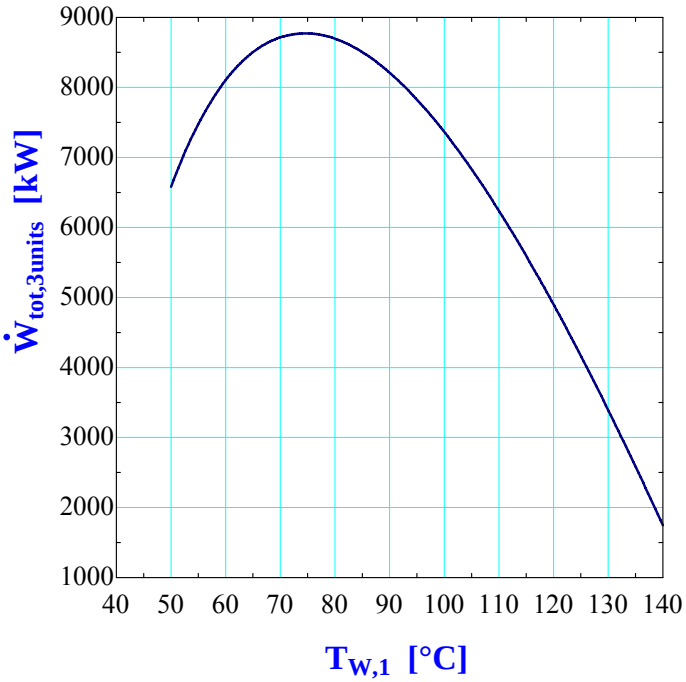

FIGURE 16: Power output vs. temperature of vaporizer outlet brine

9.4 Optimum pinch temperature of regenerator

The obtained results from calculations were plotted in Figure 17 to find the optimum pinch temperature for the regenerator. The highest power for a binary plant is attained at a pinch temperature of 1°C but the optimum pinch temperature relative to cost and power output is proportionate to 5°C. From Figure 17, it can be seen that when the

regenerator pinch temperature is 1°C, the power output is 8.3 MWe and the cost is 13.55×10^6 US$. For 5°C the power output is nearly the same, or 8.2 MWe but the cost difference is considerable, 2.35×10^6 US$.

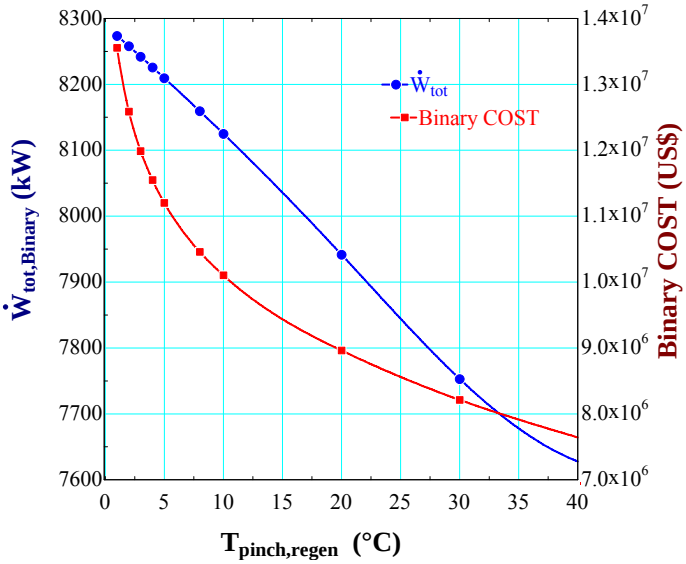

FIGURE 17: Binary power output and cost vs. regenerator pinch temperature

9.5 Optimum output of the power plant

Section 8 explained how the net power plant output is calculated by deducting the power required by the power plant from the output of the turbines. Figures 12-17 compare the power output of the plant for different operational parameters.

From Figure 12, it can be seen that the power output of the steam plant has the highest value when the separator pressure is 3 bar-a. Figure 13 shows that the power output of plants increases as separator pressure increases but the cost and also the required area for a binary plant will increase extremely with the separator pressure more than 5 bar-a. The maximum power output from plants is limited by parameters such as the steam dryness of the turbine outlet, silica deposition and especially plant cost. The optimization of operational parameters gives 26 MWe as the optimum power plant output.

10. CONCLUSIONS

The long-term target capacity of power generation in the NW-Sabalan project is about 100 MWe. There are several options for reaching this target. Steam field and power plant options at the Mt. Sabalan development site are constrained by difficulties in crossing deep and steep-sided gullies incised in the valley floor.

Well-pad B is preferred for an early development, in order to avoid the need for pipelines to cross a steep gully and unstable terrains. In this preliminary design, it has been assumed that five additional wells will be drilled and have the same properties as the existing well (NWS-4). The initial properties of the discharged fluid have, therefore, been set as input values in an EES programme and can be changed to real values when the actual output values are available.

Steam condensing with a parallel binary ORC has been selected as the power plant system in this report. Calculation and optimization of operational parameters shows that:

- A separator station should be located adjacent to the production well-pad to reduce pressure losses. The existing warehouse location and injection well-pad C were selected as the steam condensing and binary plants locations, respectively.
- The length of the steam transport pipe from separator to steam plant is fixed at 250 m, with a pressure drop of 0.01 bar. The total length of the brine transport pipe from the separator to the binary plant and re-injection wells is 2200 m, with a pressure gain of 19 bar.
- The highest power output from the steam plant is 19.5 MWe when the separator pressure is 3 bar-a and condenser pressure is 0.08 bar-a.

- The output from the steam turbine increases with lower condensing pressure but so does the power consumption of the plant. Consequently, too low a pressure in the condenser reduces the output from the power plant.
- The optimum pressure for separator and condenser is 5 and 0.1 bar-a, respectively.
- The maximum power output from the plants is constrained by parameters such as the steam dryness of the turbine outlet, silica deposition and especially plant cost.
- The optimization of operational parameters gives 26.2 MWe as the optimum power output when the power consumption of plant is about 8.5% of the turbine's generated power.

ACKNOWLEDGEMENTS

I would like to express my gratitude to Dr. Ingvar B. Fridleifsson, director, and Mr. Lúdvík S. Georgsson, deputy director, of the UNU Geothermal Training Programme for giving me the opportunity to participate in this special course and for their kindness, and to Mrs. Gudrún Bjarnadóttir for her help during the training course.

I am sincerely thankful to my supervisors, associate Professor Halldór Pálsson and Professor Páll Valdimarsson, both of the University of Iceland, for their help and advice throughout the project. Thanks to all UNU-GTP lecturers and staff members at Orkustofnun. I am thankful to SUNA - Iran for supporting me during these 6 months.

I also want to thank the UNU Fellows of 2005 for their friendship and cooperation during our training. Special thanks go to my colleague, Svetlana Strelbitskaya for her collaboration during the preparation of this report.

Finally, my deepest thanks go to my family and friends for their moral and emotional support during the six months.

REFERENCES

Armstead, H.C., 1983: *Geothermal energy* (2nd edition). J.W. Arrowsmith Ltd., Bristol, 404 pp.

Bogie, I., Cartwright, A.J., Khosrawi, K., Talebi, B. and Sahabi, F., 2000: The Meshkin Shahr geothermal prospect, Iran. *Proceedings of the World Geothermal Congress 2000, Kyushu-Tohoku, Japan,* 997-1002.

Bromley, C., Khosrawi, K., and Talebi, B., 2000: Geophysical exploration of Sabalan geothermal prospect in Iran. *Proceedings of the World Geothermal Congress, Kyushu-Tohoku, Japan,* 1009-1014.

El-Wakil, M.M., 1984: *Power plant technology.* McGraw-Hill, Inc., USA, 859 pp.

Gudmundsson, J.S., 1983: Silica deposition from geothermal brine at Svartsengi, Iceland. *Proc. Symp. Solving Corrosion-Scaling Problems in Geothermal Systems, San Francisco, Ca,* 72-87.

Kanoglu, M., 2001: *Exergy analysis of a dual-level binary geothermal power plant*. MTA, Turkey, webpage, www.mta.gov.tr/yayin/geothermics.htm.

Mineral Processing Research Institute, 2001: *The heat exchanger network (THEN) user's manual and tutorial*. MPRI, website, www.mpri.lsu.edu/Manuals%5CThenManual.PDF

Mitsubishi, 1993: *Geothermal power generation.* Mitsubishi Heavy Industries, Ltd., website, www.mhi.co.jp/power/e_power/index_f.htm.

Noorollahi, Y., and Yousefi, H., 2003: Preliminary Environmental Impact Assessment of a geothermal project in Meshkin Shahr, NW-Iran. *Proceedings of the International Geothermal Conference IGC 2003, Reykjavik*, S12, 1-11.

Perry, J.H. 1950: *Chemical engineers' handbook* (3rd ed.). McGraw Hill, NY, 1942 pp.

Sanyal, S.K., 2005: Cost of geothermal power and factors that affect it**.** *Proceedings of the World Geothermal Congress 2005**,** Antalya, Turkey,* CD*,* 10 pp.

Siregar, P.H.H., 2004: Optimization of electrical power production process for the Sibayak geothermal field, Indonesia. Report 16 in: *Geothermal Training in Iceland 2004*. UNU-GTP, Iceland, 349-376.

SKM, 2005: *NW-Sabalan geothermal feasibility study.* SUNA and Sinclair Knight Merz, draft report, 92 pp.

Talebi, B., Khosrawi, K., and Ussher, G., 2005: Review of resistivity survey from the NW Sabalan geothermal field, Iran**.** *Proceedings of the World Geothermal Congress 2005**,** Antalya, Turkey,* CD*,* 7 pp.

Valdimarsson, P., 2003: Production of electricity from geothermal heat – efficiency calculation and ideal cycles. *Proceedings of the International Geothermal Conference, IGC 200, Reykjavík,* S01 40-47.

Valero, A., Lozano, M.A., Serra, L., Tsatsaronis, G., Pisa, J., Frangopoulos, C.A. and Von Spakovsky, M.R., 1996: *CGAM* problem: definition and conventional solution. *Energy, 19*, 268-279.

APPENDIX I: Pipe design equations

a. Pipe insulation

1) $\dot{Q} = \dfrac{T_i - T_o}{\dfrac{\ln\left(\dfrac{d_o}{d_i}\right)}{2\pi k_s} + \dfrac{\ln\left(\dfrac{d_{ins}}{d_o}\right)}{2\pi k_{ins}}}$ (Heat flow from pipe to surrounding)

d_{ins} is outside diameter of insulation

k_s and k_{ins} are coefficients of thermal conductivity of steel and insulation, respectively.

$T_i - T_o$ is the temperature difference between inside of pipe and surrounding.

2) $\dot{Q}_{tot} = \dot{Q} L$ (Total heat flow)

L is the length of pipeline.

3) $\dot{Q}_{tot} = \dot{m} c_p \Delta T$ (Total heat flow)

ΔT is the temperature drop during the pipe line.

b. Pipe supports

1) $q_p = \dfrac{\pi}{4}\left(d_o^2 - d_i^2\right)\rho_s g$ (Pipe load)

ρ_s is the density of pipe.

2) $q_m = \dfrac{\pi}{4} d_i^2 \rho_m g$ (Inside fluid load)

ρ_m is the density of fluid.

3) $q_{ins} = \dfrac{\pi}{4}\left(d_{ins}^2 - d_o^2\right)\rho_{ins} g$ (Insulation load)

ρ_{ins} is the density of insulation.

4) $q_w = C\,P_w\,d_{ins}$ (Wind load)

$C = 0.6$ (Form factor of pipe)

5) $P_w = \dfrac{V_{wind}^2}{1.6}$ (Wind pressure)

V_{wind} is the velocity of wind.

6) $q_c = a\left(q_p + q_m + q_{ins}\right)$ (Seismic load)

a is the seismic factor in the area.

7) $q_{vs} = q_p + q_{ins}$ (Vertical seismic load)

8) $q_{vd} = q_m + q_s$ (Vertical dynamic load)

9) $q_{hd} = Max\left(q_w, q_c\right)$ (Horizontal dynamic load)

$0.75i = 1$ (Stress intensity factor, for straight pipe =1)

10) $k.S_h = 120\times10^6 (N/m^2)$ (Basic allowable stress during operation)

$k = 1$ (Load factor)

11) $$L_s = \left[\frac{\left(k.S_h - \dfrac{P_D\,d_o}{4\,t_p}\right)8\pi\left(\dfrac{d_o^4 - d_i^4}{32\,d_o}\right)}{0.75i\left(q_{vs} + (q_{vd}^2 + q_{hd}^2)^{0.5}\right)}\right]^{0.5}$$ (Length between supports)

P_D and t_p are the design pressure and thickness of pipe.

c. Expansion loop

1) $$L_{\exp,loop} = \left(\frac{D.\alpha.\Delta T.M}{208.3\times(2-2^{0.5})^2}\right)^{0.5}$$ (Length of expansion loop)

$\alpha = 12\times10^{-6}$ (1/°C) (Expansion coefficient of pipe)

$M = 160\times10^3$ (mm) (Distance between anchors)

Appendix II: Results diagrams from EES (Engineering Equations solver) program

1. Steam condensing diagram

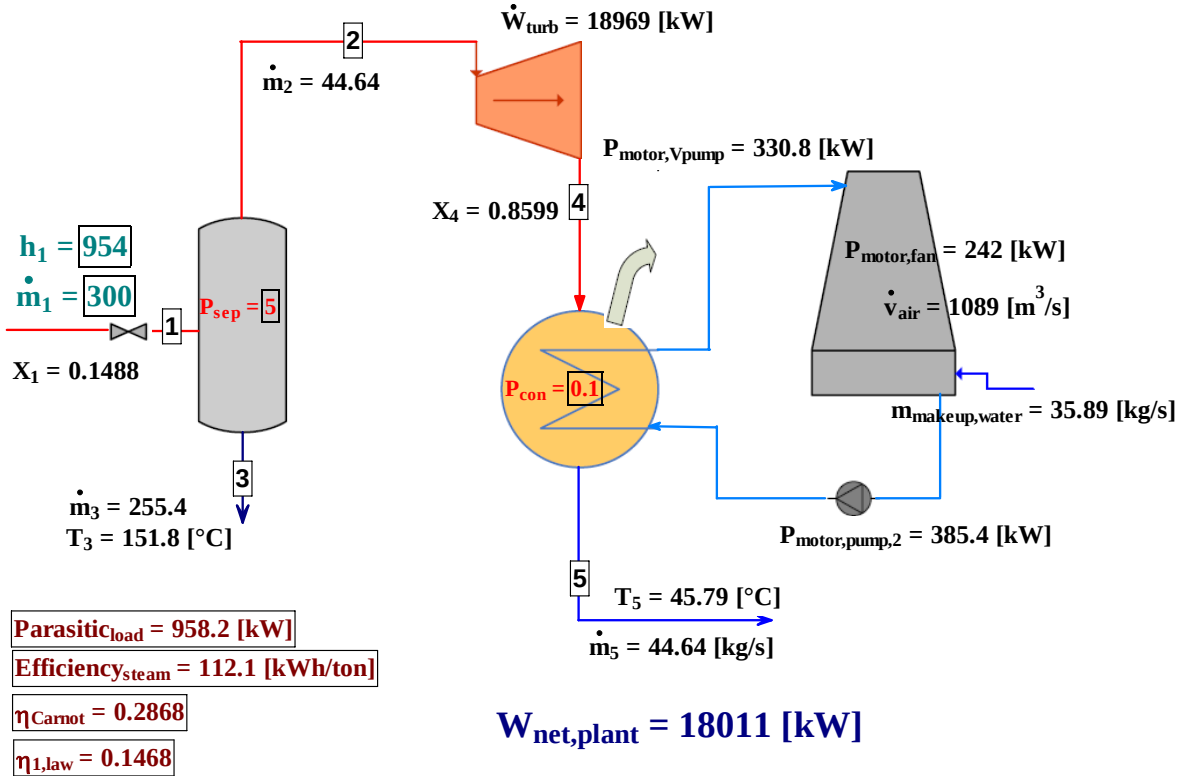

2. Binary ORC diagram